IEEE Access
Multidisciplinary | Rapid Review | Open Access Journal

Received September 28, 2017, accepted November 17, 2017, date of publication November 29, 2017,
date of current version February 14, 2018.

Digital Object Identifier 10.1109/ACCESS.2017.2778289

Uncover the Degradation Science of Silicone Under the Combined Temperature and Humidity Conditions

PREETPAL SINGH AND CHER MING TAN, (Senior Member, IEEE)
Department of Electronics Engineering, Chang Gung University, Taoyuan City 33302, Taiwan
Centre for Reliability Science and Technology, Chang Gung University, Taoyuan City 33302, Taiwan
Department of Mechanical Engineering, Ming Chi University of Technology, New Taipei City 24301, Taiwan
Chang Gung Memorial Hospital, Linkou 333, Taiwan
Institute of Radiation Research, College of Medicine, Chang Gung University, Taoyuan City 33302, Taiwan

Corresponding author: Cher Ming Tan (cherming@ieee.org)

This work was supported by the President Office of Chang Gung University by providing financial support to the CReST Laboratory.

ABSTRACT In this paper, we report the mechanistic insights into thermal and humidity induced degradation of silicone employed in high power LEDs. High power blue and white light emitting diodes (LEDs) are used for experimentation. The silicone encapsulant of both the blue and white LEDs are degraded due to hydrolysis, likewise for the molding part of the blue LED. However, the molding part of the white LED is degraded via thermal oxidation. We find that lumen degradation is rapid for white LEDs, whereas material degradation is unexpectedly rapid for blue LEDs. The reasons for such differences in the degradation of the packaging materials are explained. We also found that the degradation of LEDs under high temperature alone is different from that under high temperature and humid condition, such as those used in the outdoor applications.

INDEX TERMS Hydrolysis of silicone, oxidation of silicone, outdoor applications, FTIR, EDS, delamination, scanning acoustic microscope, optical confocal microscope, discoloration.

I. INTRODUCTION

The applications of white high power LEDs are wide spreading, and besides their general lighting applications, they are also used in outdoor applications such as head lamps in automobiles, ultra-bright large area displays, street lamps, park lamps, to name a few.

There are several elements in a packaged high power LED namely molding part, heat sink, LED chip, die attach, lead frame, encapsulant, Au wires for bonding and lens as shown in Figure 1.

Silicone based materials are considered to be the most appropriate materials for encapsulant, molding part and lens of LED due to their wide range of advantages such as suitable refractive index of 1.4–1.57, good UV and thermal resistance, low-impurity levels, good moisture resistivity, high-optical clarity, and low modulus [1], [2].

Silicone function as molding part for the housing material in LEDs due to its mechanical strength and its enhancement on light output because of its reflector shape and special filler addition [3].

Silicone based packaging has replaced thermoplastic based pre-molded packaging in the LED industry as thermoplastic based molding packaging is more pronounced to surface yellowing (browning) and detachment of encapsulant under high temperature exposure, which renders shorter lifetime of packaged LEDs [4]–[6]. Silicone manufacturer for LEDs such as CAPLINQ can now prepare silicone for molding part, encapsulant as well as lens [6]. Silicone is essential for the LED packaging industry today.

Generally, silicone can be considered as a ''molecular hybrid'' between glass and organic linear polymers [7], [8]. The chemical structure of silicone is $[R_2SiO]_n$, where an inorganic Si-O backbone is bonded with an organic group R such as methyl or phenyl as shown in Figure 2. Physical properties of silicone, namely hardness, refractive index or gas/humidity permeability can be altered by varying the Si-O chain length, side group R selection and crosslinking methods [4]. According to Joon-Soo Kim [5], two different types of silicone, namely poly dimethylsiloxane and phenylsiloxane as shown in Figure 2, are mixed in different

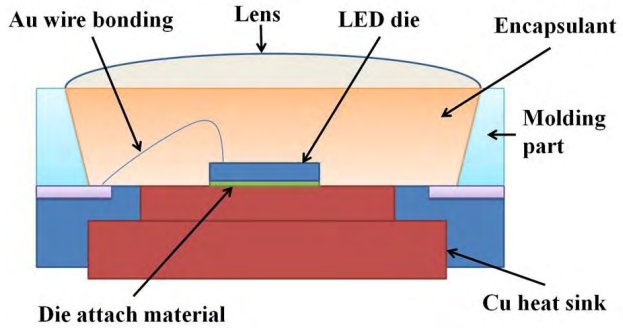

FIGURE 1. Schematic cross-sectional view of a SMD LED package.

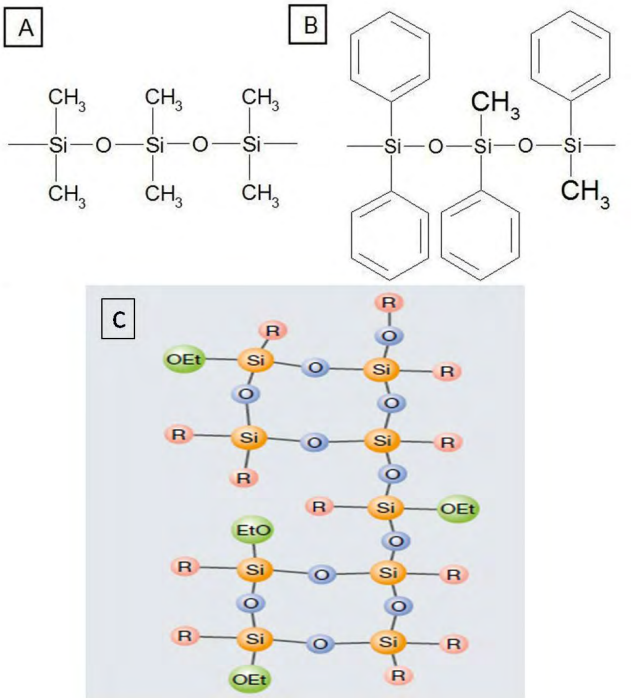

FIGURE 2. Two examples of silicone used in LED packaging: (A) dimethylsiloxanes and (B) phenylsiloxanes. (C) Silicone resins for molding part in LEDs. In Figure 2(c), R stands for CH_3 and OEt stands for Oxy Ethyl groups [5].

concentrations for different functions in a LED package. Sela *et al.* [9] shows that the molding part of LEDs can be prepared by silicone resins which consists of highly branched polymer structures as shown in Figure 2 (C).

During the operation of high power LEDs, their chip temperature can go up to 135°C with high intensity light output up to 80 lumens [10]. Hence, thermal/photo degradation of silicone at high temperatures were studied where the alteration of its chemical structure were investigated as reported in [11]–[14]. This change in the chemical structure of silicone leads to degradation in its physical properties such as mechanical strength, color change and transparency [7]. For example, the irreversible oxidation reactions under high temperature, such as methyl side group oxidation, can result in CH_2-CH_2 cross linking between two silicone backbones, causing an increase in the silicone hardness and induce cracks in the material [15].

For LEDs employed in outdoor environment, moisture is a common stress factor to the degradation of LED packages [16]. This moisture, together with high temperature due to the heat generated in the LED chip, could modify the degradation processes of silicone. Singh and Tan [10] found that the degradation mechanisms for blue and white LEDs when tested under high temperature and high humidity conditions are different. Moisture plays a significant role in blue LED's degradation whereas the heat produced by the phosphor in white LEDs leads to the reduction of moisture, and delamination at the encapsulant and molding part interface was found to be the mechanism for the white LED degradation. Zhang et al observed that the package of mid power LEDs showed yellowing under thermal moisture stress and such yellowing did not observe when LEDs are tested under only thermal stress alone [17]. In summary, the degradation mechanisms of silicone under thermal only and thermal-moisture conditions are different.

While silicone degradation under high temperature and high humidity condition is the obvious cause of lumen degradation, the underlying science of the silicone degradation due to the combined effect of temperature and humidity is still unknown, and this is the focus of this work. FTIR spectroscopy and EDS will be used to understand the chemical changes occurring in the various LED parts.

II. EXPERIMENTATION

Two sets of high power OSRAM golden dragon LEDs are chosen, each consists of 20 units of white high power LEDs and blue high power LEDs respectively. All the LEDs are subjected to 85°C/85%RH environmental condition in a temperature- humidity chamber (μ series from Isuzu), and 350 mA constant current is passing through them individually, according to the manufacturing specification. Their electrical measurements are done using Keithley source meter model 2651A, and their optical measurements are done with system comprises of a 1-m-diameter integrating sphere model SLM-40TS-110902 and a spectro-radiometer model Ocean Optics QE6500. Initial set of measurements are done for all of them to serve as reference baseline for each test sample.

The samples are taken out of the humidity-temperature chamber in every 24-hours interval for their optical and electrical measurements. The setting for all the measurements is done according to [18] to prevent self-heating during measurement. All the measurements are done within 3 hours from the time the samples are taken out from the test chamber in order to keep the moisture out-diffusion from the packages to the lowest. Optical microscope Keyence VHX5000 is used to examine the LEDs' packages after each test interval. SONIX UHR-2001 Scanning acoustic microscope (SAM) is also employed to examine the delamination in the packages.

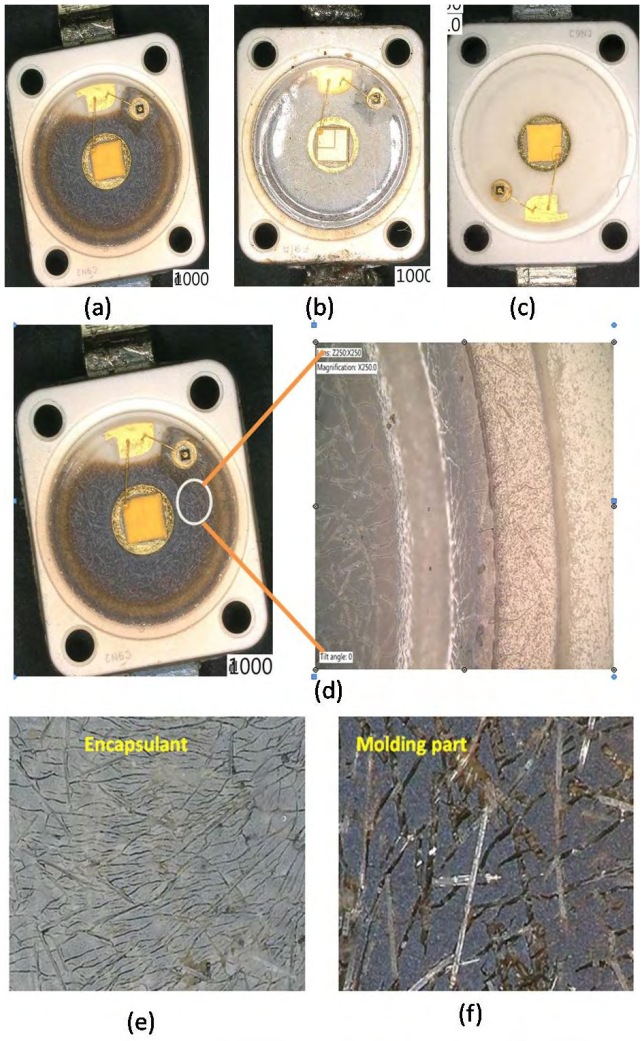

FIGURE 3. Optical micrograph of silicone discoloration in (a) white LEDs tested for 144 hours, (b) blue LEDs tested for 356 hours respectively when compared to (c) fresh LEDs. (d) A closer look of the top view of the degraded white LED. Encapsulant and molding parts are also detached from one another for detail examination. Optical micrographs at 500 X magnification of (e) Encapsulant and (f) molding part of degraded white LEDs tested under 85 °C / 85% RH and ON condition for 144 hours.

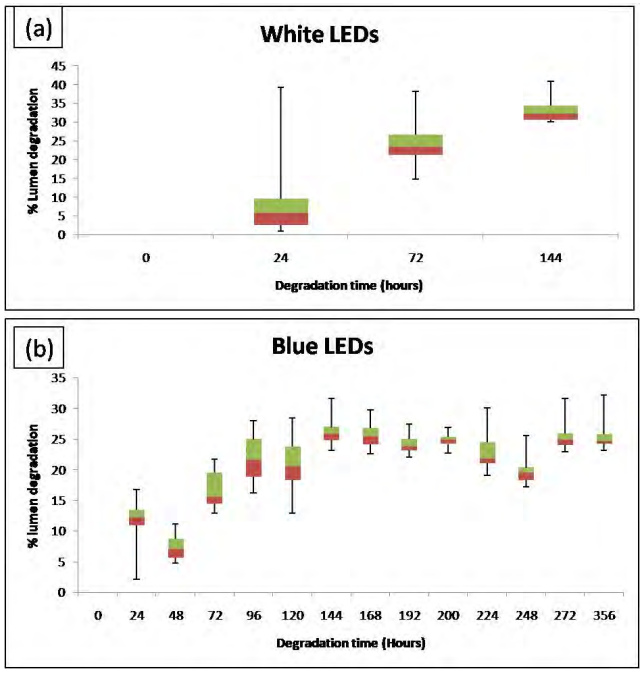

FIGURE 4. Percentage lumen degradation from 20 samples observed for (a) white and (b) blue LEDs after testing.

III. EXPERIMENTAL RESULTS

Discoloration is observed vividly for the degraded blue LEDs tested for 356 hours when compared to the fresh LEDs as seen in Figure 3. The discoloration is worse in the case of the degraded white LEDs tested for only 144 hours when compared to the blue LEDs tested for 356 hours. The white LEDs reached 33% lumen degradation in 144 hours, whereas the blue LEDs took 356 hours to reach 25 % lumen degradation as shown in Figure 4.We stopped the tests for both the sets according to ASISST standard [19] which sets the largest acceptable lumen degradation at 30%.

The discoloration observed in LEDs could either be due to the degradation of encapsulation material or the molding part material. This discoloration has a direct impact on the light output of the LEDs. As the test conditions are the same for both the white and blue LEDs, i.e. 85 °C and 85 % RH and both LEDs have the same type of dice, the more severe discoloration of white LEDs as compared to the blue LEDs suggest that the heat generated from the phosphor in white LEDs is mostly likely the main cause for the more severe discoloration in white LEDs than the blue LEDs. This phosphor is used to convert the blue light from the dice to yellow light so that a white light is produced through the combination of the blue and yellow lights. This light production process is also accompanied with the heat generation which can lead to the overall increase in temperature, renders the LED molding part and encapsulant degradations as found by Singh and others [20]–[22].

As it is unclear from the top view of the LED shown in Figure 3(d) that the observed discoloration is either due to encapsulant and/or molding part, they are detached so that a separate investigation of the encapsulant and molding part degradation can be done. Figure 3(e) and (f) show their optical micrographs using degraded white LED as example.

Figure 3(e) and (f) show that cracks are uniformly distributed over the entire surface of the encapsulant and the molding part for the white LEDs, but the crack features are different. Therefore, the degradation mechanism of the encapsulant and the molding parts of LEDs under the temperature-humidity test are likely to be different. To probe further into the different mechanisms, 3D Confocal microscope is used along with SEM to observe the cracks and their topology, and EDS is used to see the elemental composition change in the encapsulant and molding part before and after the test. The analysis results are described below.

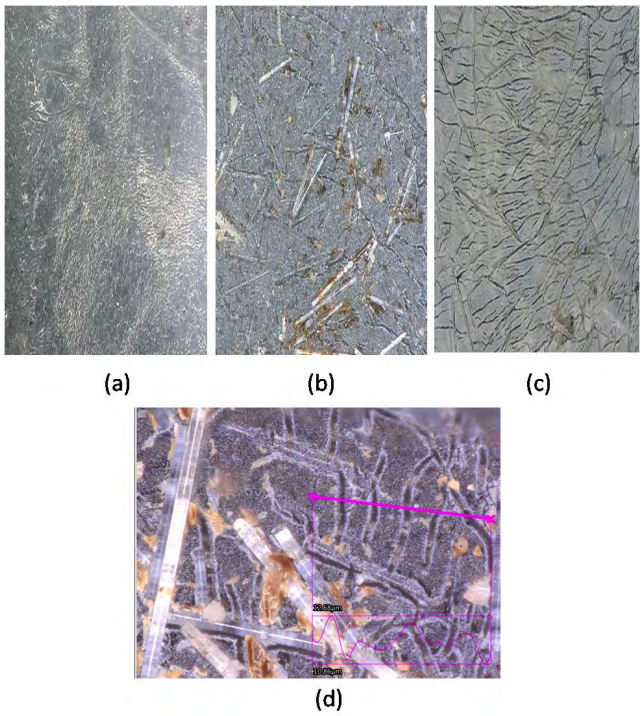

FIGURE 5. Optical microscope images at 200 x magnification of silicone encapsulant for (a) Fresh sample, (b) degraded Blue LED (tested for 356 hours), and (c)degraded white LED (tested for 144 hours). (d) Crack depth measurement on the encapsulant for degraded blue LEDs.

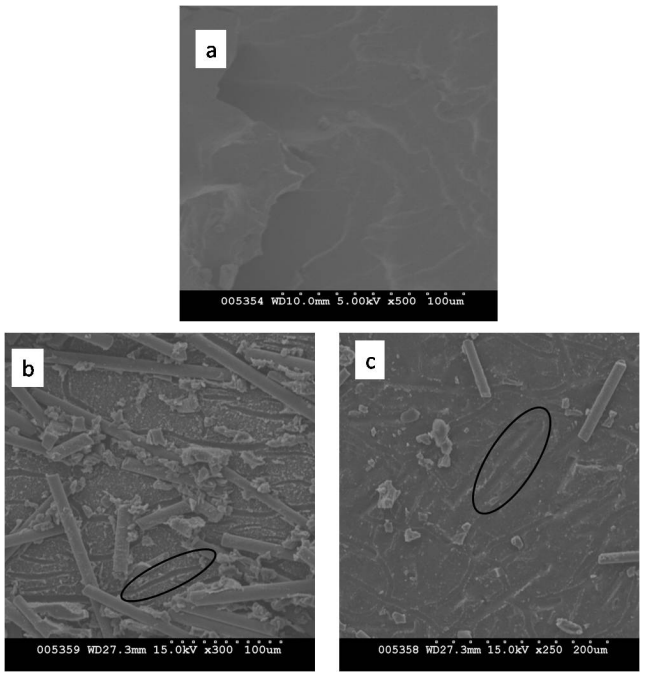

FIGURE 6. SEM images of (a) Fresh, (b) blue degraded and (c) white degraded encapsulant. Crack lines are shown by black circles in (b) and (c).

A. DEGRADATION OF ENCAPSULANT

Figure 5 shows the detailed optical images of the encapsulant of the LEDs, and one can see that the surface of the encapsulant of the fresh LED is reasonably smooth. However, cracks are observed on both the degraded LEDs. Flakes (or tube) like structures are present only on the encapsulant of the degraded blue LEDs. The crack depth on the encapsulant of the blue and white LEDs is found to be very small. The maximum crack depth observed for blue degraded LED encapsulant is 3 μm as shown in Figure 5(d) and that for white degraded LED encapsulant is almost negligible and not able to measure using optical microscope.

SEM is used to get a closer look on the surface of the blue and white degraded LED's encapsulant when compared with a fresh LED encapsulant. The SEM images of the surface topology of the encapsulant before and after degradation for both the LEDs are shown in Figure 6. It is observed from Figure 6 that there are small cracks present on the encapsulant surfaces of both the degraded LEDs when compared with the fresh sample, which is consistent with their optical micrographs. However, flake like structures are more evident on the blue degraded LEDs surface as compared to the white degraded LEDs. We will explore the origin of flakes or tube like structures on the degraded surfaces later.

Both SEM and optical micrographs shows that the crack density and crack depth are higher in the case of blue LED's encapsulant than the white LED. However, the percentage lumen degradation for the blue LEDs is less than that of the white LEDs. As there is higher amount of heat generation due to the phosphor converting the blue light to yellow light as mentioned earlier, more cracks should be expected for the white LEDs, but this is not consistent with the micrographs obtained in our work. We will discuss the observations later in the discussion section.

To further understand the nature of the cracks, Energy dispersive system (EDS) is employed to examine the cracks surface of the degraded and fresh encapsulants, and the results are shown in Table 1 where it shows an increase in the oxygen content for both the degraded LEDs. The increase in oxygen is higher in the case of the blue degraded LED's encapsulant as compared to that of the white LEDs.

To further understand the reason behind the increase of oxygen content for the degraded LEDs, FTIR spectroscopy is employed as shown in Figure 7(a).

On closer examination of the FTIR results shown in Figure 7(a), it is observed that new peaks (shown inside the red circle) are found for the blue degraded encapsulant in the region from 3000 to 3500 cm^{-1}. This region corresponds to -OH peaks as shown in Figure 7(b) [23], [24], implying that the degraded blue LED encapsulants have undergone hydrolysis process. White degraded LED's encapsulant shows very small -OH peaks (almost negligible), indicating weak hydrolysis mechanism occurring in the encapsulant of the white LEDs, and this is expected as moisture is mostly driven away by the heat generated from the phosphor layer in white LED as mentioned earlier. The higher amount of hydrolysis can also explain the increase in oxygen content in the EDS results for both the degraded LEDs, with the blue LED being the most significant.

TABLE 1. Chemical composition data by EDS for the encapsulant of fresh sample, blue and white degraded samples.

	Atomic %		
Element	Fresh	Blue degraded	White degraded
Carbon	45.72	47.95	46.2
Oxygen	30.86	42.84	35.85
Silicon	23.42	9.21	17.95

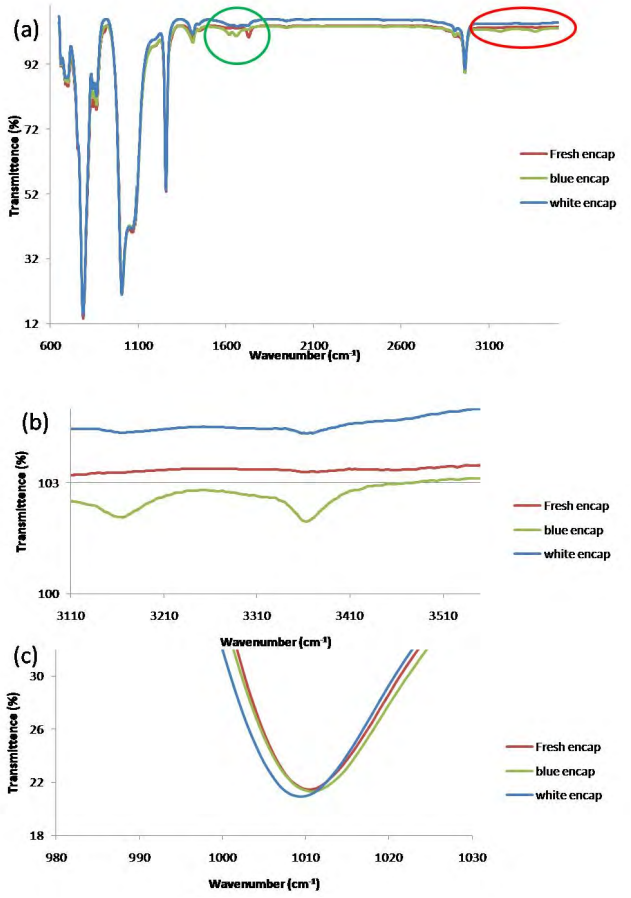

FIGURE 7. (a) FTIR spectroscopy result for fresh, blue degraded and white degraded LED's encapsulant. (b) FTIR results for –OH peak for fresh and degraded samples encapsulant (c) FTIR results for Si-O-Si peak for fresh and degraded samples encapsulant.

On the other hand, very little amount of oxidation is observed in the degraded blue and white LED encapsulant samples as shown in Figure 7(c) as evident from the negligible change in peak position. As the heat generated in blue LED is less than that in the white LED, only 1.48% change in the transmittance of the Si-O-Si peak is observed in the blue LEDs Si-O-Si peak in comparison to the 2.7% of that in the white LEDs.

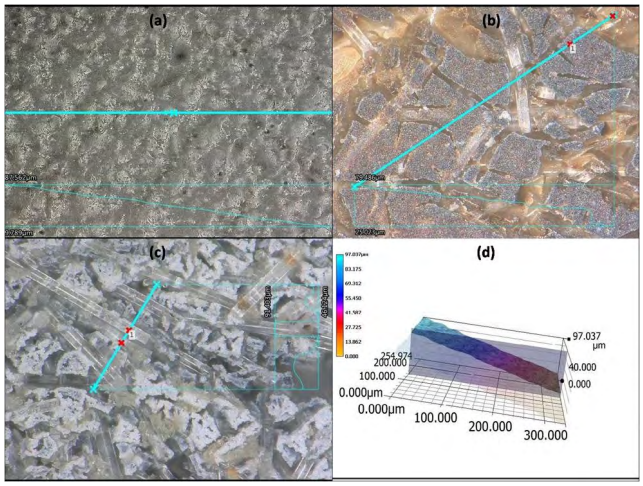

FIGURE 8. 2-D microscopic images of the surface of the silicone molding part for (a) fresh LED, (b) white degraded LED and (c) blue degraded LED, taken at 1000 x magnification. (d) The Depth profile images of the fresh LED surface as example for depth measurement. The color spectrum shows the height of cracks at different places.

Green circle in Figure 7(a) represents C = O peaks which could arise either due to environmental carbon dioxide presence or from the oxidation reaction. As it is observed that very little amount of oxidation took place in the degraded encapsulant, these peaks are likely the result of environmental CO_2.

B. MOLDING PART DEGRADATION

Figure 8 shows the 3D optical images of the cracks and discoloration developed on the surface of the molding part where crack depths are measured using Keyence VHX5000 optical microscope. The nature of cracks is different for the blue and white degraded LEDs. The cracks on the blue LEDs are short, denser and deeper as compared to the cracks on the white LEDs. Given that the test time for the blue LEDs is 356 hours, and the average crack depth is 43.63 μm, the average crack propagation rate is 0.11μm/hour. On the other hand, for the white LEDs where the test time is 144 hours, and the average crack depth is 23.59 μm, the average crack propagation rate is 0.16 μm/hour, indicating that the degradation in the White LEDs is more severe than that in the Blue LEDs with regards to the molding part degradation and thus the lumen degradation, unlike the case of encapsulant degradation, although both of them are silicone.

Figure 8(c) shows that the blue LED molding surface has more flakes/tube like structures when compared with the white degraded LED's molding part. SEM images of the molding parts are shown in Figure 9, and one can clearly observe that the molding surface of the blue degraded LED is completely converted into flakes or tube like structures as shown in Figure 9(b).Tube like structures are shown in the rectangular box whereas flakes like structures are shown in the circular box in Figure 9(b). In the case of white degraded

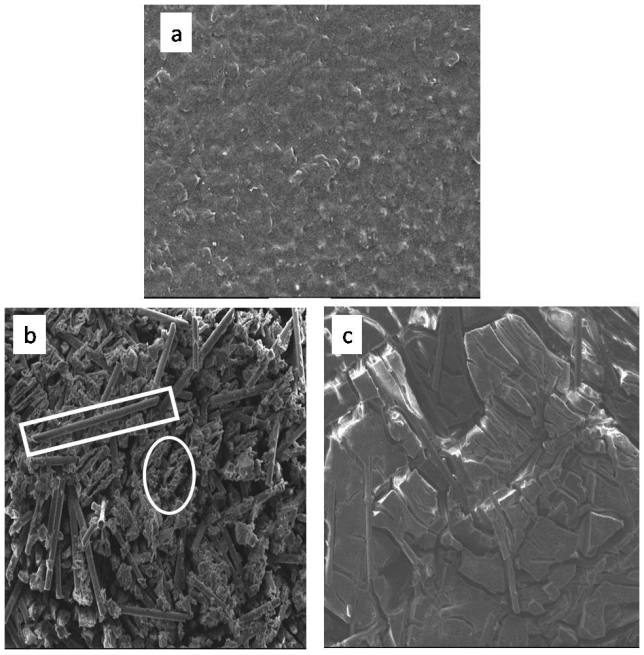

FIGURE 9. SEM images of (a) Fresh, (b) blue degraded and (c) white degraded molding part. Tube like structures are shown in a rectangular box whereas flakes like structures are shown in a circular box in Figure 9(b).

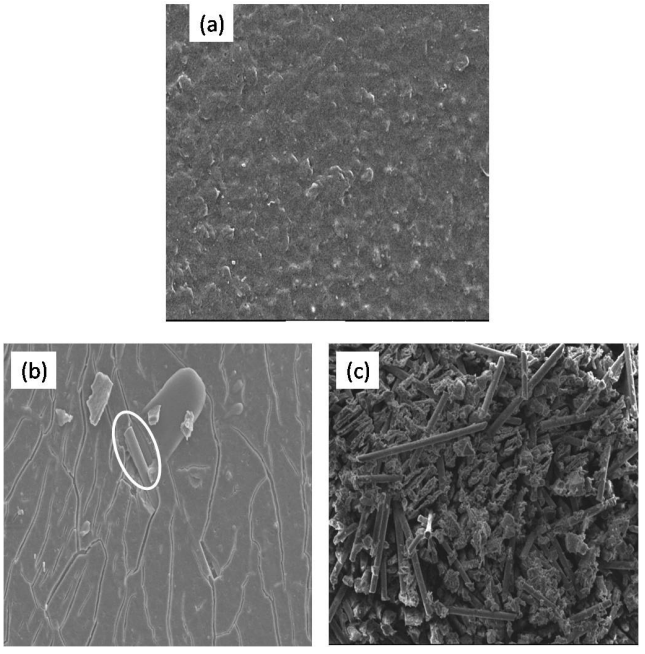

FIGURE 10. SEM images of blue LED's molding part after degradation time of (a) 0 hours i.e. fresh sample, (b) 144 hours and (c) 365 hours. Circle in Figure (b) represents the formation of tube like structures from the cracks on the molding part of degraded blue LED.

LEDs, only cracks and few tube-like structures are observed on the molding surface as seen in Figure 9(c).

It has been reported that when the length of a crack exceeds a critical value, surface fracture in the form of flakes-like and hill-like structures will occur [25], [26]. The value of the critical crack length depends on the free energy or elastic energy of the material under stress, and it is the length beyond which free energy decreases as the crack length increases, thereby causing fracture [27]. As cracks could only be seen on the surfaces of white LEDs' molding part, and the testing time for the white LEDs is shorter, in comparison to the blue LEDs where flake-like and tube-like structures are found on the surfaces of their molding part, we propose that the long testing duration of the blue LEDs could have rendered the surface cracks length beyond the critical value.

Additional experiment is thus performed to confirm this proposal where three blue LED samples were tested under the same conditions for an intermediate time (144 hours as compared to our original test time of 365 hours for blue LEDs), and the typical surface is observed under SEM as shown in Figure 10. It is observed from Figure 10 that the molding part after 144 hours is similar to the surface of the white degraded LEDs, supporting our proposal. This implies that the critical crack length occurs between 144 and 356 hours. Further time dependent experiments will be necessary to determine the exact time at which the molding part reaches its critical crack length during this high temperature humidity stress conditions, but it is beyond the scope of this work.

Energy dispersive system (EDS) is used to assess the elemental composition of the molding part and the results are shown in Table 2 where it shows that the carbon content

TABLE 2. Chemical composition data by EDS for the molding part of fresh sample, blue and white degraded samples.

	Atomic % composition%]		
Element	Fresh	Blue degraded	White degraded
Carbon	77.53	49.14	54.23
Oxygen	21.91	41.85	38.88
Silicon	0.56	9.01	6.89

decreases and oxygen content increases for the degraded LED's molding part as compared to the fresh samples. The oxygen content is found to be higher in blue degraded LEDs molding part as compared to the white degraded LED's molding part, similar to the case of the encapsulant.

Thermal oxidation process of silicone during testing could lead to the oxidation of the pendant groups, i.e. methyl groups attached to Si in the silicone structure, thereby leading to the rise in O content and proportionally decrease in C content as shown by Akihiko, et al and other groups [15], [28]. After thermal degradation, the proportion of Si increases due to the outward diffusion of oligomer as shown by Zhou *et al.* [28]. Oligomers are the complex molecules consisting of simple monomer units, for example polyethylene is an oligomer

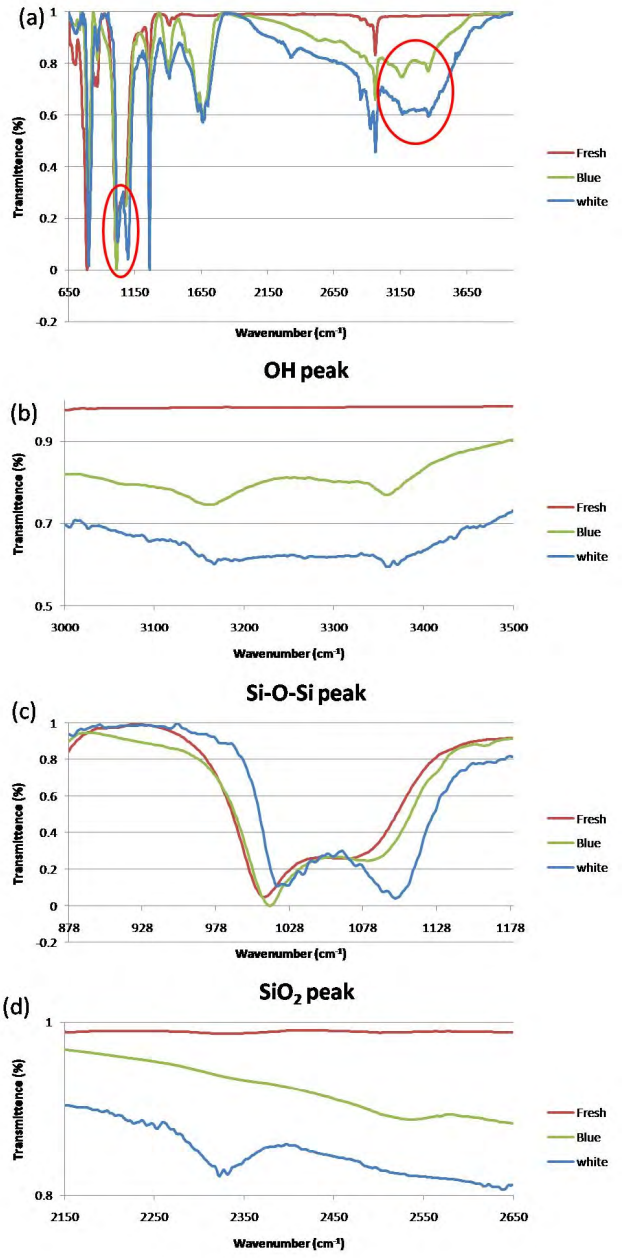

FIGURE 11. FTIR spectroscopy result for (a) fresh, blue degraded and white degraded LED's molding part, (b) -OH peaks, (c) Si-O-Si peaks and (d) CO_2 peak observed for degraded LEDs.

consisting of monomer named as polyethylene gas as a precursor. However, hydrolysis can also lead to increase in oxygen content apart from oxidation process as mentioned earlier in the encapsulant degradation study. Thus FTIR spectroscopy is employed as it is also done for encapsulant. FTIR spectroscopy results for degraded and fresh molding part are shown in Figure 11(a).

Higher amount of hydrolysis is observed for the blue degraded LED molding part when compared to white as shown in Figure 11(b). Higher hydrolysis peaks could be due to higher testing time or lower amount of heat generated

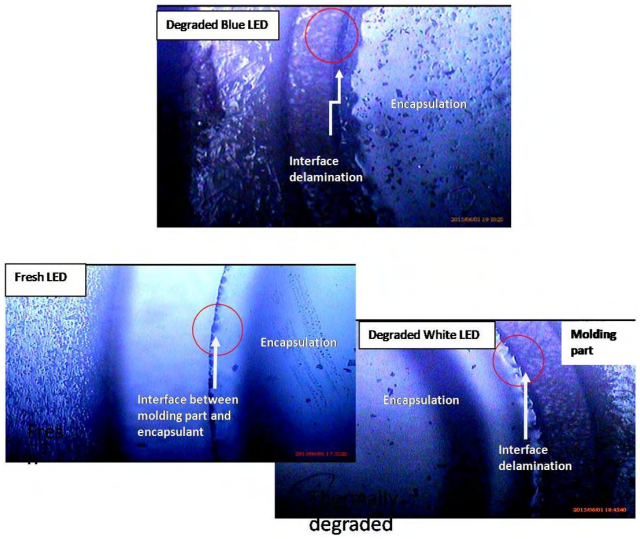

FIGURE 12. Optical micrographs of the molding part-encapsulant interface at 5x magnification, showing the delamination induced in (a) blue degraded LEDs, (b) fresh LED and (c) white degraded LED.

in blue LEDs when compared with white LEDs. However, a sharp and new peak arises at 1098 cm^{-1} for the white degraded LED molding part, indicating that it has undergone higher oxidation, and there is insignificant change in the peak shape or position for the blue degraded LED molding part when compared with fresh sample. A small CO_2 peak at 2321 cm^{-1} for the degraded white LED shown in Figure 11(d) is likely a by-product of thermal oxidation reaction as shown by Huang and Wang[29] and Stepkowska [30]. The CO_2 peak is not present for the blue degraded LED samples. In other words, the molding part degradation mechanism is different for blue and white LEDs in contrast to the case of encapsulants. Degradation of white LEDs molding part is due to oxidation whereas that of blue LEDs molding part is due to hydrolysis. The peak at 1655 cm^{-1} represents the amide group presence on the degraded samples as shown by previous literature [31], however, the cause of its presence in our results is yet to be found out.

IV. DISCUSSION

The reasons for the different mechanisms reported in the above-mentioned can be traced to the structure of the LEDs. The LED molding part and encapsulant are made up of different silicone materials with different thermal expansion coefficients, and this could lead to hydrostatic stress at the interface of encapsulant and molding part during high temperature testing [10]. This hydrostatic stress could lead to interface delamination at the molding part-encapsulant interface.

Optical micrographs of the molding part-encapsulant interfaces for the LEDs are shown in Figure 12. Figure 12 shows that the cracks are developed all along the outer edges of molding part- encapsulant interface for degraded LEDs. The delamination is observed to be larger for the degraded white LEDs than the degraded blue LEDs as the temperature of

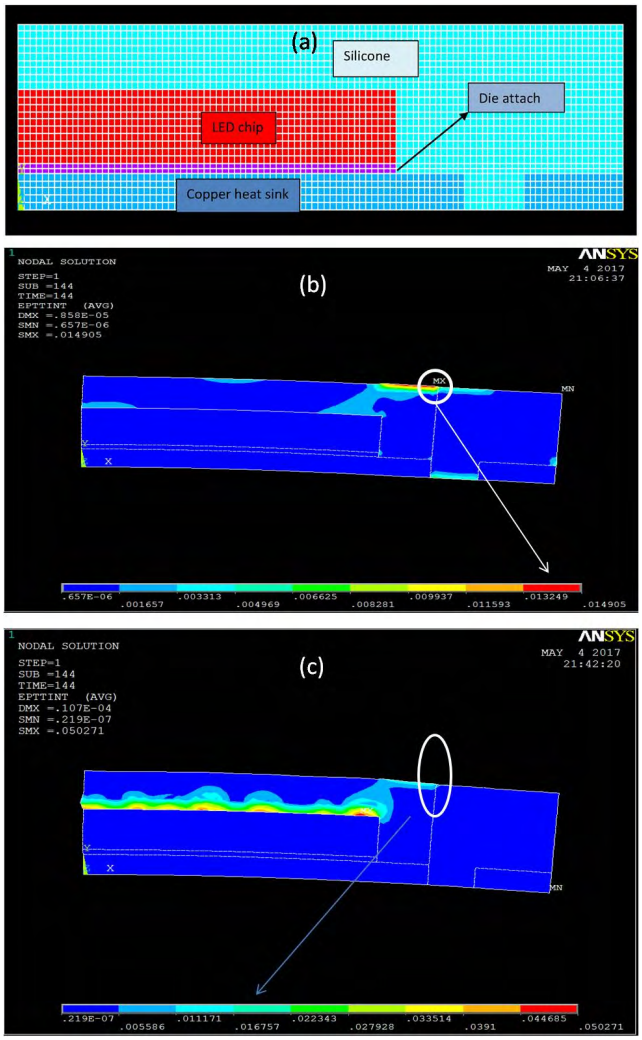

FIGURE 13. FEM using ANSYS showing (a) the structure of LED used for simulation and thermo-mechanical strain in case of (b) blue LED and (c) white LED after thermal humidity test. Circular region and arrows indicating the amount of thermo-mechanical strain observed in that region.

the white LED is higher due to the heat generated from the phosphor layer in the white LED. The fresh sample shows no cracks at the interface.

Finite element analysis (FEM) using ANSYS software is employed to compute the stress distribution in the LEDs' package during 85°C/85%RH testing, and the results are shown in Figure 13. Thermo-mechanical properties of the silicone materials were used from the work done by Zeng *et al.* [32]. The ambient temperature is kept at 85 °C and the LED temperature is measured using thermal IR camera and found to be 95 °C for blue LEDs. The white LEDs internal temperature reached 135 °C due the phosphor heat generation [10].

Figure 13 clearly shows the thermo-mechanical strain distributions in the LEDs, and one can see that the strain at the molding part-encapsulant interface for the degraded white LED is 0.167 which is larger than that of the blue LED

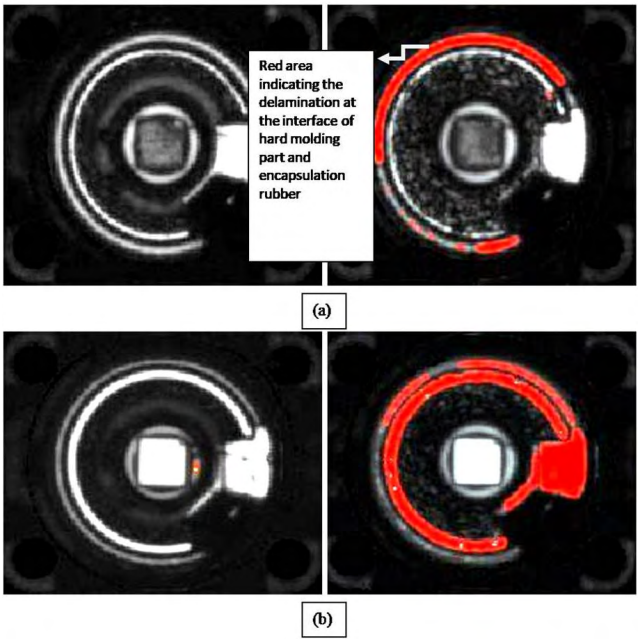

FIGURE 14. C-SAM images show the delamination at interface between silicone encapsulant and molding part of (a)WHITE LEDs and (b) BLUE LEDs. The red area shows the locations of the detachment when the samples are exposed to high humidity and high temperature exposures. The left hand side figure shows the fresh LED's C-SAM image and right hand side figure is the degraded LED's C-SAM image. The chip area can be identified easily by a square exactly at the center of the LED package.

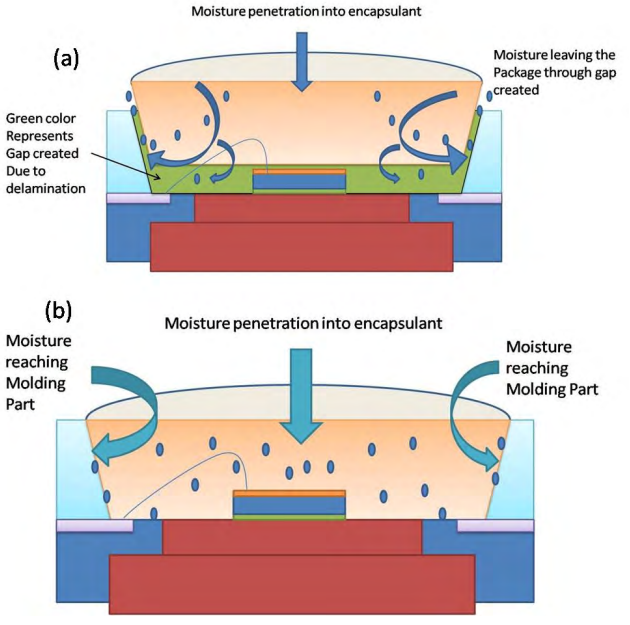

FIGURE 15. Moisture penetration pattern in (a) white degraded LEDs and (b) blue degraded LEDs.

where strain is 0.149, as indicated in the circular region and arrows of Figure 13. These results are consistent with our optical microscope results shown in Figure 12. Also, the thermo-mechanical strain is much larger at the encapsulant-chip interface for the white LED.

For further confirmation, C-SAM is performed and the results are shown in Figure 14. The C-SAM results show that the delamination, which is shown as red color region, is higher for white LED at the outer most edges whereas it is higher in the internal parts for blue LEDs, consistent with our FEA results. Also, for the white LED, the delamination also occurs in the chip area, which is consistent with our FEA results where delamination is expected between the encapsulant-chip interface.

The severe delamination at the encapsulant-molding part interface of the degraded white LED can also be felt when the encapsulant is pulled out from the molding part manually, and the effort needed for the degraded white LED is the least.

The delamination at the chip-encapsulant interface also renders lesser heat transfer from the dice to the encapsulant in the case of white LED, unlike the blue LEDs, and hence one can observe lower degradation for white LED's encapsulant as compared to the degraded blue LEDs as discussed previously.

These results also consistent with our EDS and FTIR results for degraded encapsulant reported earlier where we observed higher hydrolysis for blue degraded LED's encapsulant when compared to the white degraded LED's encapsulant. This delamination also reduced the severity of thermal oxidation on the encapsulant for the white LEDs, and hence only very small cracks can be seen in the encapsulant of the degraded white LEDs as shown in Figures 3 and 6.

The severe delamination of the encapsulant-molding part interface in the degraded white LEDs, together with its higher heat generated in the phosphor layer render easy evaporation of moisture as shown by a schematic in Figure 15 (a), and this evaporation prevents hydrolysis reaction in the white LEDs encapsulant and the molding part. Thus, no OH peaks were found in white degraded LED's encapsulant and the molding part. However, the higher temperature in the degraded white LED's molding part lead to the discoloration of the molding part and higher cracks propagation rate as a result of severe thermal oxidation as observed in FTIR results shown in Figure 11.

Thermal oxidation has a significant impact on the white LED molding part as discoloration reduces the light reflection effectiveness of molding part, and also the gap created at the molding part and encapsulant interface reduces the overall light output coming out from the degraded white LEDs as shown by Luo *et al.* [33]. Owing to the above mentioned phenomena, higher lumen degradation is observed for white LEDs in a very short span of testing time.

The encapsulant in blue degraded LEDs is not completely detached from the molding part which led to the entrapment of moisture in the encapsulant or the flow of moisture from encapsulant to other parts of LED such as molding part and die attach as shown by schematic in Figure 15(b).

On the other hand, the heat generated in blue LEDs is much less than the white LEDs and this prevents moisture from evaporating outwards. Hence new OH peak is observed only for blue degraded encapsulant and molding part as discussed earlier. The lower heat generation in blue LED also reduces the degree of thermal oxidation as observed in our FTIR results. This suggests that the moisture is the reason for the surface fracture on the molding and encapsulant surface of the blue degraded LEDs. These are also observed by others [34], [35].

V. CONCLUSION

In this work, the sciences of silicone degradation used as encapsulant and molding part under high temperature and high humidity conditions are identified, and their effects on the performances of high power blue and white LEDs are studied. The interfacial stress between the two silicones used as encapsulant and molding part due to their differential coefficient of thermal expansion is found to be responsible for the difference degradation mechanisms observed in white and blue LEDs. We found that hydrolysis process of the encapsulant and molding part silicone is the degradation mechanism for the blue LEDs, and oxidation process of the silicone of the molding part is the degradation mechanism of the white LED. The encapsulant of the white LED has very slight degradation and it is due to hydrolysis process.

Lumen degradation is found to be higher for white LEDs whereas the material degradation is higher for blue LEDs. This seemingly contradicting but interesting observation is attributed to the structure of the LED and the delamination of the encapsulant-molding part interface.

This work also shows that the degradation mechanism of LEDs due to temperature-humidity condition is different from that due to temperature alone. Hence, for outdoor or high humidity applications of LEDs, Moisture-electrical-temperature test as proposed by Singh and Tan [10] is needed.

ACKNOWLEGDMENT

The authors wish to acknowledge the suggestions provided by Prof. T. E. Soon from National University of Singapore.

REFERENCES

[1] Y.-H. Lin, J. P. You, Y.-C. Lin, N. T. Tran, and F. G. Shi, "Development of high-performance optical silicone for the packaging of high-power LEDs," *IEEE Trans. Compon. Packag. Technol.*, vol. 33, no. 4, pp. 761–766, Dec. 2010.

[2] R. D. Dupuis and M. R. Krames, "History, development, and applications of high-brightness visible light-emitting diodes," *J. Lightw. Technol.*, vol. 26, no. 9, pp. 1154–1171, May 1, 2008.

[3] J. P. You, N. T. Tran, Y.-C. Lin, Y. He, and F. G. Shi, "Phosphor-concentration-dependent characteristics of white LEDs in different current regulation modes," *J. Electron. Mater.*, vol. 38, no. 6, pp. 761–766, Jun. 2009.

[4] G. Lin, Y. Zhou, N. Tran, W. Chiang, Y. He, and F. G. Shi, "Materials Challenges and Solutions for the Packaging of High Power LEDs," in *Proc. 11th Int. Symp. Adv. Packag. Mater., Process., Properties Interface*, Mar. 2006, p. 63.

[5] J.-S. Kim, S. Yang, and B.-S. Bae, "Thermally stable transparent sol–gel based siloxane hybrid material with high refractive index for light emitting diode (LED) Encapsulation," *Chem. Mater.*, vol. 22, no. 11, pp. 3549–3555, Jun. 2010.

[6] K.-J. Byeon, J.-Y. Cho, J. O. Song, S. Y. Lee, and H. Lee, "High-brightness vertical GaN-based light-emitting diodes with hexagonally close-packed micrometer array structures," *IEEE Photon. J.*, vol. 5, no. 6, Dec. 2013, Art. no. 8200708.

[7] J. A. Semlyen and S. J. Clarson. (1993). *Siloxane Polymers*. Englewood Cliffs, NJ, USA: Prentice-Hall. Accessed: Sep. 11, 2017. [Online]. Available: https://www.pearson.com/us/higher-education/program/Clarson-Siloxane-Polymers/PGM15393.html

[8] R. H. Baney, M. Itoh, A. Sakakibara, and T. Suzuki, "Silsesquioxanes," *Chem. Rev.*, vol. 95, no. 5, pp. 1409–1430, Jul. 1995.

[9] Y. Sela, S. Magdassi, and N. Garti, "Polymeric surfactants based on polysiloxanes—Graft-poly (oxyethylene) for stabilization of multiple emulsions," *Colloids Surfaces A, Physicochem. Eng. Aspects*, vol. 83, no. 2, pp. 143–150, Mar. 1994.

[10] P. Singh and C. M. Tan, "Degradation physics of high power LEDs in outdoor environment and the role of phosphor in the degradation process," *Sci. Rep.*, vol. 6, no. 1, 2016, Art. no. 24052.

[11] G. Camino, S. M. Lomakin, and M. Lageard, "Thermal polydimethylsiloxane degradation. Part 2. The degradation mechanisms," *Polymer*, vol. 43, no. 7, pp. 2011–2015, Mar. 2002.

[12] J. Zhang, S. Feng, and Q. Ma, "Kinetics of the thermal degradation and thermal stability of conductive silicone rubber filled with conductive carbon black," *J. Appl. Polymer Sci.*, vol. 89, no. 6, pp. 1548–1554, Aug. 2003.

[13] R. N. Lewis, "Methylphenylpolysiloxanes," *J. Amer. Chem. Soc.*, vol. 70, no. 3, pp. 1115–1117, Mar. 1948.

[14] N. Grassie and I. G. Macfarlane, "The thermal degradation of polysiloxanes—I. Poly(dimethylsiloxane)," *Eur. Polymer J.*, vol. 14, no. 11, pp. 875–884, Jan. 1978.

[15] A. Shimada, M. Sugimoto, H. Kudoh, K. Tamura, and T. Seguchi, "Degradation mechanisms of silicone rubber (SiR) by accelerated ageing for cables of nuclear power plant," *IEEE Trans. Dielectr. Electr. Insul.*, vol. 21, no. 1, pp. 16–23, Feb. 2014.

[16] P. Singh and C. M. Tan, "A review on the humidity reliability of high power white light LEDs," *Microelectron. Rel.*, vol. 61, pp. 129–139, Jun. 2016.

[17] J. Huang *et al.*, "Degradation mechanisms of mid-power white-light LEDs under high-temperature—Humidity conditions," *IEEE Trans. Device Mater. Rel.*, vol. 15, no. 2, pp. 220–228, Jun. 2015.

[18] C. M. Tan and P. Singh, "Time evolution degradation physics in high power white LEDs under high temperature-humidity conditions," *IEEE Trans. Device Mater. Rel.*, vol. 14, no. 2, pp. 742–750, Jun. 2014.

[19] M. Y. Mehr, W. D. van Driel, K. M. B. Jansen, P. Deeben, and G. Q. Zhang, "Lifetime assessment of Bisphenol—A Polycarbonate (BPA-PC) plastic lens, used in LED-based products," *Microelectron. Rel.*, vol. 54, no. 1, pp. 138–142, Jan. 2014.

[20] D. Mingzhi, W. Jia, Y. Huaiyu, Y. Cadmus, and Z. Kouchi, "Thermal analysis of remote phosphor in LED modules," *J. Semicond.*, vol. 34, no. 5, p. 053007, May 2013.

[21] M.-H. Chang, D. Das, P. V. Varde, and M. Pecht, "Light emitting diodes reliability review," *Microelectron. Rel.*, vol. 52, no. 5, pp. 762–782, May 2012.

[22] N. Narendran, Y. Gu, J. P. Freyssinier, H. Yu, and L. Deng, "Solid-state lighting: Failure analysis of white LEDs," *J. Crystal Growth*, vol. 268, nos. 3–4, pp. 449–456, 2004.

[23] G. Beshkov, S. Lei, V. Lazarova, N. Nedev, and S. S. Georgiev, "IR and Raman absorption spectroscopic studies of APCVD, LPCVD and PECVD thin SiN films," *Vacuum*, vol. 69, nos. 1–3, pp. 301–305, Dec. 2002.

[24] E. Yilgör, E. Yurtsever, and I. Yilgör, "Hydrogen bonding and polyurethane morphology. II. Spectroscopic, thermal and crystallization behavior of polyether blends with 1,3-dimethylurea and a model urethane compound," *Polymer*, vol. 43, no. 24, pp. 6561–6568, Nov. 2002.

[25] J. P. Berry, "Determination of fracture surface energies by the cleavage technique," *J. Appl. Phys.*, vol. 34, no. 1, pp. 62–68, Jan. 1963.

[26] D. Maugis, "Subcritical crack growth, surface energy, fracture toughness, stick-slip and embrittlement," *J. Mater. Sci.*, vol. 20, no. 9, pp. 3041–3073, Sep. 1985.

[27] D. B. Marshall, B. R. Lawn, and A. G. Evans, "Elastic/plastic indentation damage in ceramics: The lateral crack system," *J. Amer. Ceram. Soc.*, vol. 65, no. 11, pp. 561–566, Nov. 1982.

[28] Y. Zhou, Y. Zhang, L. Zhang, D. Guo, X. Zhang, and M. Wang, "Electrical tree initiation of silicone rubber after thermal aging," *IEEE Trans. Dielectr. Electr. Insul.*, vol. 23, no. 2, pp. 748–756, Apr. 2016.

[29] N. Huang and J. Wang, "A TGA-FTIR study on the effect of $CaCO_3$ on the thermal degradation of EBA copolymer," *J. Anal. Appl. Pyrol.*, vol. 84, no. 2, pp. 124–130, Mar. 2009.

[30] E. T. Stepkowska, "Simultaneous IR/TG study of calcium carbonate in two aged cement pastes," *J. Thermal Anal. Calorimetry*, vol. 84, no. 1, pp. 175–180, Apr. 2006.

[31] A. Pawlak and M. Mucha, "Thermogravimetric and FTIR studies of chitosan blends," *Thermochim. Acta*, vol. 396, nos. 1–2, pp. 153–166, Feb. 2003.

[32] P. Zeng, D. Yang, H. Tang, and M. Cai, "Hygro-thermo-mechanical modeling of LED Luminaires," in *Proc. 14th Int. Conf. Electron. Packag. Technol.*, Aug. 2013, pp. 606–611.

[33] X. Luo, B. Wu, and S. Liu, "Effects of moist environments on LED module reliability," *IEEE Trans. Device Mater. Rel.*, vol. 10, no. 2, pp. 182–186, Jun. 2010.

[34] R. L. Feller. (1995). *Accelerated Aging: Photochemical and Thermal Aspects*. Los Angeles, CA , USA: Getty Publications. Accessed: Sep. 11, 2017. [Online]. Available: https://books.google.com.tw/books?hl=en&lr=&id=wp1OAgAAQBAJ&oi=fnd&pg=PP1&dq=Accelerated+aging:+photochemical+and+thermal+aspects&ots=8QgzbMAgrL&sig=6m1UxGyjvTwtUDdFlVLraRphb1s&redir_esc=y#v=onepage&q=Acceleratedaging%3Aphotochemicalandthermal

[35] E. Chiellini, A. Corti, S. D'Antone, and R. Baciu, "Oxo-biodegradable carbon backbone polymers—Oxidative degradation of polyethylene under accelerated test conditions," *Polymer Degradation Stability*, vol. 91, no. 11, pp. 2739–2747, Nov. 2006.

PREETPAL SINGH was born in Jammu and Kashmir, India, in 1989. He received the B.S. degree from the Guru Nanak Engineering College, Hyderabad, India, in 2007, and the M.S. degree from Amity University, Noida, India, in 2013. He is currently pursuing the Ph.D. degree with the Department of Electronic Engineering and the Semiconductor Laboratory, Chang Gung University, Taoyuan, Taiwan. His research interests include graphene-based high power LEDs, high power LED degradation study, and LED reliability.

He has published his research in reputed journals like the IEEE-TDMR, *Microelectronics Reliability*, and *Scientific Reports*. He is also the Reviewer for the IEEE-TDMR and microelectronics journals.

CHER MING TAN (M'84–SM'99) received the Ph.D. degree in electrical engineering from the University of Toronto, Toronto, ON, Canada, in 1992. He has ten years of experience in reliability of the electronic industry in Singapore and Taiwan before joining Nanyang Technological University (NTU), Singapore, where he has been a Faculty Member from 1996 to 2014. He has published over 300 international journal and conference papers and holds 11 patents and one copyright for reliability software. He was the Chair of the IEEE Singapore Section, the Director of SIMTech-NTU Reliability Laboratory, and a Senior Scientist with SIMTech, A*Star. He is a senior member of the American Society for Quality, a Distinguished Lecturer of the IEEE Electron Devices Society on Reliability, the Founding Chair of IEEE Nanotechnology Chapter. Singapore Section, a Fellow of The Institution of Engineers Singapore, a Fellow and an Executive Council Member of Singapore Quality Institute. He is the Founding Chair of the IEEE International Nanoelectronics Conference. He is currently the Director of the Center for Reliability Sciences and Technologies, a Professor with the Department of Electronic Engineering, College of Engineering, and the Institute of Radiation Research, College of Medicine of Chang Gung University, Taiwan. He is also the Chair Professor in mechanical engineering with the Ming Chi University of Technology, Taiwan. He is also a Researcher with the Department of Urology, Chang Gung Memorial Hospital, Taiwan, the European Frequency and Time Forum Award, the Carl Zeiss Research Award, the William F. Meggers Award and the Adolph Lomb Medal. He is an Editor of the *Scientific Report*, *Nature Publishing Group*, an Editor of the IEEE TRANSACTIONS ON DEVICE AND MATERIALS RELIABILITY, the Guest Editor of the *International Journal of Nanotechnology*, *Nanoscale Research Letters*, and *Microelectronic Reliability*. He is also the Series Editor of *Springer Briefs in Reliability.*